Low energy (10 to 700 eV) angularly resolved sputtering yields for D^+ on beryllium

1998 Nucl. Fusion 38 673

(http://iopscience.iop.org/0029-5515/38/5/303)

LOW ENERGY (10 TO 700 eV) ANGULARLY RESOLVED SPUTTERING YIELDS FOR D^+ ON BERYLLIUM

P.C. SMITH, D.N. RUZIC
Department of Nuclear Engineering,
University of Illinois at Urbana-Champaign,
Urbana,
Illinois,
United States of America

ABSTRACT. The phenomenon of ion induced sputtering is integral to many applications. In magnetically confined fusion, this sputtering is important for both the lifetime of the plasma facing components and the contamination of the plasma. A method has been developed to obtain both the angular distribution and the total sputtering yield. The total yield is determined by collecting the sputtered material on a quartz crystal microbalance. The sputtered material is also collected on a pyrolytic graphite collector plate. By mapping the concentrations of the sputtered material on this plate, both the polar and the azimuthal angular distribution can be determined. Utilizing this set-up, data have been obtained for 10 to 700 eV D^+ on beryllium at a 45° angle of incidence to the normal. Subthreshold sputtering (0.004 ± 0.003 at 10 eV) has been observed. These data are some of the first to become available, especially at the lower energies.

1. INTRODUCTION

In fusion experiments and test reactors, the choice of materials for the first wall and divertor are crucial [1, 2]. High-Z materials such as tungsten show very little erosion. However, even low levels of these materials in the plasma lead to an intolerable decrease in the energy confinement times of the device owing to bremsstrahlung radiation [3, 4]. Of the low-Z materials, beryllium and graphite are the leading candidates. Although graphite has a lower physical sputtering yield, it is also prone to highly temperature dependent chemical sputtering, in which it reacts with hydrogen to create hydrocarbons (e.g., CH_4) [5, 6]. When these effects are taken into account the total yield equals or exceeds that of beryllium. For these reasons, beryllium has already been installed and tested in JET for its plasma facing components [7], and it is proposed as the first wall material for ITER [8, 9].

Most of the available sputtering measurements are not taken from surfaces that realistically match the surface conditions that would be encountered in a real device. In situ measurements on JET of D^+ on beryllium sputtering is ideal in that it uses the real conditions. Unfortunately lack of control over the experimental conditions and dependence on spectroscopy make these measurements very difficult. Those that have been done indicated that the "sputtering yield is 6–30%, which is much higher than expected from the experimental data" [10]. There are numerous reasons why these laboratory experimental yields do not match the estimates in JET. One of these is that the beryllium surfaces in a tokamak will be loaded with deuterium, which can affect the yields [11–13]. Laboratory measurements should endeavour to reproduce tokamak conditions but usually do not. Most ion beam driven experiments that determine the sputtering through weight loss measurements [14] do not mimic the surface in a tokamak, nor do they measure the angular distribution of the sputtered material needed for transport calculations [15]. Plasma simulator results [16] only produce measurements of the yield integrated through an assumed transport model that is dependent on the plasma sheath, magnetic field and other conditions unique to the specific simulation device. These experiments are also prone to contamination with carbons, hydrocarbons, oxides, oxygen, water and nitrogen [10].

The existing database of D^+ on beryllium sputtering yields consists almost entirely of one group's work at six energies from 27 to 1000 eV and only 14 data points. Of these points, 12 are at normal incidence and the other two are at an energy of 300 eV at 45 and 50° to the normal [17]. Although some older data are available [18], the energies involved are greater than 1 keV and the surfaces do not reflect the conditions in a fusion plasma. Therefore, the data from Ref. [17] stand alone as the only experimental data, apart from

numerous computer simulations and theoretical models in recent reviews of the subject [19–22].

The need for more data at these lower energies, then, is a vital component for a better understanding of the mechanisms involved and for validation of the theoretical and computational models already in use. An apparatus has been developed to measure low energy angularly resolved sputtering yields [23]. This apparatus and method allows beryllium samples to be sputtered and 'filled' by the bombardment of D^+ in situ, prior to the determination of their angularly resolved sputtering yield. The absolute yield, as well as the polar and azimuthal angularly resolved yields, of the sputtered flux can be determined as a function of ion energy and angle of incidence for 10 eV to 1 keV ions.

While our initial results of D^+ on beryllium at higher energies have been published previously [24], this article expands and revises that work to lower energies, compares it with all the other data and explains the analysis in detail. In this article, the experimental apparatus, independent computer modelling and experimental results are described. The implications for the erosion and surface tritium inventory of ITER or other fusion experiments are covered in other works [25, 26].

2. THEORY AND MODELLING

Despite the problems in applying linear cascade theory to the systems of interest here, analytical formulas based on a linear cascade can have a great deal of success when coupled with experimental data and appropriate scaling factors are chosen [19]. In 1984 Bohdansky used Sigmund's analytic sputtering theory to derive a usable analytic formula for the sputtering yield as a function of the incident ion's energy at normal incidence. This formula is known consequently as the 'Bohdansky formula' [27],

$$Y(E_0, \alpha = 0^\circ) = Q s_n^{TF}(\epsilon) \left[1 - \left(\frac{E_{th}}{E_0}\right)^{2/3}\right] \left(1 - \frac{E_{th}}{E_0}\right)^2 . \quad (1)$$

It is plotted along with the experimental points in Section 5.

Computer simulations have also been used to predict the sputtering coefficients. Two of the most successful have been the binary collision codes TRIM [28] and TRIM.SP [29]. A three dimensional fractal model for surface roughness has been added to the basic TRIM framework as well as an improved low energy non-binary collision model. This code is called VFTRIM-3D and has several versions. VFTRIM-3D.v25 includes a mechanism for channelling energy from subsurface layers to the top layer while VFTRIM-3D.v26 does not. A thorough discussion of this code can be found in Ref. [30]. Additional information is available in Ref. [31].

In all of these codes there exist adjustable parameters. For low energy studies the surface binding energy (SBE) and the energy needed to break a bond in the bulk of the material (BE) are two of the most critical. For beryllium the measured bulk value for SBE is 3.36 eV. Standard procedure is to take BE = 0.1SBE. However, molecular dynamic simulations show that the binding energies of atoms on surface protrusions can be 1 to 2 eV lower than those from the smooth parts of a surface [32]. In addition, when a top-most atom sputters there is no need to consider a separate bond energy. The best fit to the experimental data was achieved with VFTRIM-3D.v26 with SBE = 2.26 eV and BE = 0.0 for energies less than 100 eV and VFTRIM-3D.v25 with SBE = 3.36 and BE = 0.34 for energies greater than 100 eV. At 100 eV the values from the two codes overlapped.

The surface modelled consisted of 25% deuterium and 75% beryllium, a ratio of 0.33 D/Be. The saturation of deuterium in beryllium was shown by Wampler [33] to be 0.31 D/Be and by Kawamura et al. [34] to be 0.36 D/Be at room temperature. To simulate transport through a magnetized sheath where the direction of the magnetic field is a few degrees off being parallel to the surface, D^+ ions were incident at a 45° angle. Chodura [35] showed that angles near 45° from normal are the most likely impact angles of light ions. The results of these runs provided the energy and angular distributions of the sputtered atoms. They are shown in Section 5.

3. EXPERIMENTAL APPARATUS

An ion beam is generated in a Colutron plasma based ion source [36, 37]. It is then accelerated and focused at an energy of 700 eV by a three element cylindrical electrostatic lens. The proper charge to mass ratio is then selected as the beam transits an $\boldsymbol{E} \times \boldsymbol{B}$ filter. The focused and species selected beam passes next into the ultrahigh vacuum (UHV) chamber. The electrostatic repulsive force between the ions in the beam acts to spread the beam and decrease its intensity. The beam is transported at an energy

of 700 eV, so that the velocity of the ions is fairly high as they transit the system from source to target and the time of this interaction is minimized (10 ms). The deceleration of the beam to the desired energy and final focus is therefore performed as close to the target as possible. Here, this is accomplished by a five element cylindrical electrostatic lens that was modelled with the SIMION3D [38] program. After transiting the decelerator, an electrostatic filter removes the neutral component from the beam immediately prior to the beam striking the target.

In order to simulate the surface conditions of an actual device more closely, the samples were sputtered in situ with a D^+ plasma. This was accomplished by moving a small (1 cm by 2 cm) hollow cathode plasma source in front of the −350 V negatively biased target for 20 min. The measured ion current to the sample was 0.4 mA/cm^2, enough to remove one monolayer every 7.7 s. This will remove surface oxides since the base pressures of water vapour and oxygen have a partial pressure of the order of 10^{-9} torr. Though the flux of D^+ is ∼3 orders of magnitude below that expected at a divertor, the exposure is ∼3 orders of magnitude longer, giving a similar fluence and saturating the material. The beryllium is S-65 C grade, supplied by the Brush–Wellman Company. It came from lot 4763 and was machined to 32 microinch RMS or better without EDM and then etched in a 2–2–2 solution.

A schematic diagram of the data collection apparatus is shown in Fig. 1. The collector plate is a grade ZYH pyrolytic graphite monochromator manufactured by Advanced Ceramics Corporation and is 12 mm by 12 mm square. Pyrolytic graphite was chosen as a collector for two reasons. First, being highly planar, the graphite readily formed extremely flat surfaces. By carefully applying a piece of ordinary adhesive tape to the surface, a new layer can easily

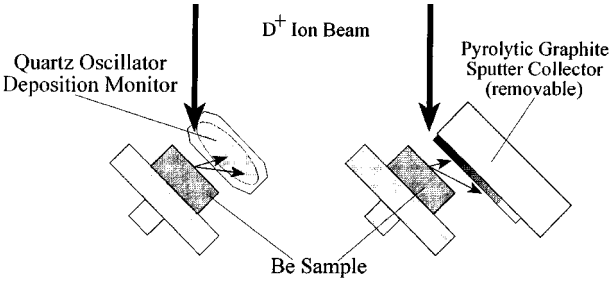

FIG. 1. Details of sputter data collection apparatus with a D^+ ion beam incident on a beryllium sample at 45° to the normal.

be cleaved when the tape is removed. Auger analysis of the collector plates after this cleaving, but without any deposited films, showed them to be remarkably free of contaminates. In fact, no other elemental lines are in evidence on the scan, including oxygen, which is often difficult to avoid. The second reason for choosing pyrolytic graphite is that the Auger line of carbon (275 eV) is very distinct from the oxygen (510 eV) and beryllium (108 eV) lines that were of interest in this study. After the target has been sputtered, the collector plate is removed from the vacuum and transferred to a PHI 660 Auger spectrometer. The transfer is carried out in air, which allows the beryllium to oxidize, though that oxidation should already have occurred in the chamber, as will be described. The surface concentrations of beryllium and oxygen are then determined to obtain the distribution.

Also pictured in the figure is the arrangement of the quartz crystal oscillator (QCO). Although both the collector plate and the quartz crystal oscillator are mounted on the manipulator, the measurements are not simultaneous. The collector plate measurement is made and is immediately followed by that of the quartz crystal oscillator. It is difficult to determine the total sputtering yield from the collector plate data alone. The reasons for this include difficulties in modelling the surface film as well as reflection and resputtering. These effects conspire to indicate a value that is much lower than the actual yield. Fortunately, these effects affect the collector plate nearly uniformly so that the areal densities obtained can be accurately compared with one another to obtain an angular distribution; however, this distribution cannot be accurately integrated to obtain the total yield.

A QCO microbalance was incorporated into the apparatus to allow for an independent measure of the total sputtering yield. Before the ion beam hits the target, a baseline frequency is determined from the QCO over a period of several hours. After an exposure to the beam for several hours, another wait of several hours is monitored to determine the total thickness. The time after the exposure is required to allow full oxidation of the deposited beryllium from the background O_2 and H_2O. Indeed, the QCO frequency rises for some time after the beam has been turned off. The frequency finally stabilizes and this is the frequency used to determine the weight of the deposited material. The amount of beryllium is then calculated assuming that the film consists of BeO. Non-sticking of beryllium, resputtering from reflected neutrals and the incorporation of deuterium are also taken into account using the same procedure as described in

Ref. [24]. The final value obtained from the microbalance is then used to scale the distribution from the collector plate so that when integrated, it gives the proper total yield [39].

4. DATA ANALYSIS

To determine the areal density of sputtered material on the collector plate merely taking the intensity distribution of the Auger signal will not suffice. Owing to the difference in transparency of the primary electrons through the material and other factors, a more detailed analysis is required.

The differential of the intensity from a pure sample (such as the carbon of the collector plate) would be [40]

$$\mathrm{d}I_\mathrm{A} = \kappa' S'_\mathrm{A} N_\mathrm{A} \exp\left(-\frac{x}{\lambda_\mathrm{A}^\mathrm{A}\cos(\phi)}\right)\mathrm{d}V$$

where $\mathrm{d}I_\mathrm{A}$ is the intensity of the Auger electron spectroscopy (AES) peak of material A from element $\mathrm{d}V$, κ' are variables dependent upon the instrument alone (such as the detection efficiency and X ray flux), S'_A variables dependent upon the material (such as photoelectron (Auger) production efficiency and electron mean free paths), N_A is the atomic density of material A, x is the distance below the surface, λ_A^β is the mean free path of emitted electrons of energy corresponding to the peak associated with element A travelling through material β and ϕ is the angle of the electron detector with respect to the surface normal ($\phi = 0$).

In areas where the deposited beryllium layer is several monolayers thick, we must account for the shielding of this signal by the deposited film. Adding this shielding term, and noting that the cosine term is 1, the equation becomes

$$\mathrm{d}I_\mathrm{A} = \kappa' S'_\mathrm{A} N_\mathrm{A} \exp\left(-\frac{x}{\lambda_\mathrm{A}^\mathrm{A}}\right)\exp\left(-\frac{t}{\lambda_\mathrm{A}^\mathrm{B}}\right)\mathrm{d}V$$

where t is the thickness of the layer. We set $\mathrm{d}V = \mathrm{d}A\,\mathrm{d}x$ and integrate over the volume of the sample,

$$I_\mathrm{A} = \int_\infty^0 \kappa' S'_\mathrm{A} N_\mathrm{A} \exp\left(-\frac{x}{\lambda_\mathrm{A}^\mathrm{A}}\right)\exp\left(-\frac{t}{\lambda_\mathrm{A}^\mathrm{B}}\right)\Delta A\,\mathrm{d}x.$$

Since the area illuminated by the electron beam (ΔA) will be the same for all intensities, we can absorb ΔA into κ such that $\kappa = \kappa'\Delta A$. Integrating, we obtain,

$$I_\mathrm{A} = \kappa S'_\mathrm{A} N_\mathrm{A} \lambda_\mathrm{B}^\mathrm{A} \exp\left(-\frac{t}{\lambda_\mathrm{B}^\mathrm{A}}\right).$$

Rather than determining absolute measurements of the mean free paths and the other material dependent parameters, signals from each element are compared and related to a standard material. These material specific parameters are then contained in the sensitivity factors ($S_\mathrm{A} = S'_\mathrm{A}\lambda_\mathrm{A}^\mathrm{A}$). For the Auger spectrometer the standard is the silver line,

$$I_\mathrm{A} = \kappa S_\mathrm{A} N_\mathrm{A} \exp\left(-\frac{t}{\lambda_\mathrm{B}^\mathrm{A}}\right).$$

For material deposited near the surface of the collector plate the derivation is similar but we integrate x from 0 to t rather than from 0 to infinity. For this case,

$$I_\mathrm{B} = \kappa S_\mathrm{B} N_\mathrm{B}\left[1 - \exp\left(-\frac{t}{\lambda_\mathrm{B}^\mathrm{B}}\right)\right].$$

The ratio of these equations is then taken,

$$\frac{I_\mathrm{A}}{I_\mathrm{B}} = \frac{S_\mathrm{A} N_\mathrm{A}}{S_\mathrm{B} N_\mathrm{B}} \frac{\exp\left(-\frac{t}{\lambda_\mathrm{B}^\mathrm{A}}\right)}{\left[1 - \exp\left(-\frac{t}{\lambda_\mathrm{B}^\mathrm{B}}\right)\right]}.$$

The values of all the terms on the right hand side of this equation are readily available: the sensitivity factors, S_B and S_A, are tabulated for the PHI 660 Auger spectrometer, the peak to peak data mentioned earlier, I_B and I_A, the atomic density of pyrolytic graphite, N_B, and the mean free path of the emitter Auger electrons, $\lambda_\mathrm{B}^\mathrm{B}\lambda_\mathrm{B}^\mathrm{A}$.

This equation is transcendental, but it can be solved numerically for the individual data points using an iterative algorithm. Once t is known, this value is converted into an areal density n_B using the following relation: $n_\mathrm{B} = tN_\mathrm{B}$.

Table I. Total Yield Measurements for D^+ Ions Incident on Beryllium at 45° to the Normal

Energy (eV)	Yield	
	Experiment	VFTRIM-3D
10	0.004 ± 0.003	0.00153
20	0.012 ± 0.009	0.0119
50	0.025 ± 0.008	0.0367
100	0.066 ± 0.005	0.063
300	0.099 ± 0.007	0.112
500	0.111 ± 0.009	0.121
700	0.118 ± 0.009	0.115

5. RESULTS

The total sputtering yield for the D^+ on beryllium experiments and the VFTRIM-3D simulations are shown in Table I. The fractal dimension used for the VFTRIM-3D runs was 2.05 with 2.5×10^5 incident particles. The experimental conditions are described in detail in Section 3. These data are plotted in Fig. 2.

The angular distribution data are shown in Fig. 3. There is no angular distribution figure for the 10 eV point. At that energy the only portion of the collector plate that showed any detectable amount of beryllium was the $\Theta = 0°$ analysis area. The amount of material deposited onto the QCO in this case was too small to allow for the calculation of a total yield from this measurement. The correction factor for 50 eV was used in this case to scale the data, since the variation of the correction factors is at most 2%. This assumption and the fact that the distribution is not well represented by a single area of the collector plate resulted in the 75% error bars for this point. The significance of this 10 eV point is discussed in the following section. Table II shows the parameter n when the data are fitted to a $\cos^n(\Theta)$ distribution. The distribution is undercosine ($n < 1.0$) for lower energies and approaches a cosine distribution ($n = 1.0$) at higher energies.

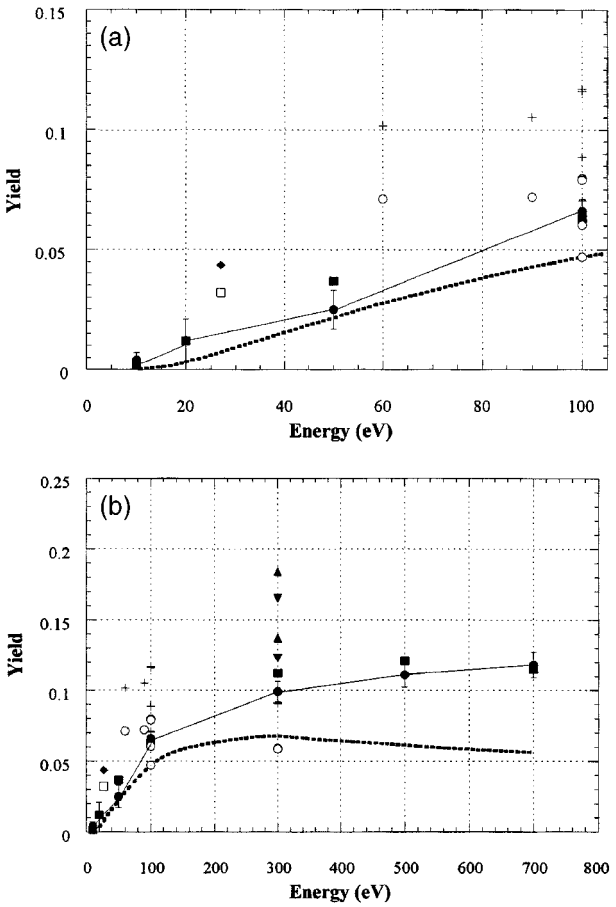

FIG. 2. Total yield measurements for D^+ on beryllium: (a) low energy range, (b) full energy range. Data: full curve with closed circles, experimental data from Ref. [17]; dashed curve, empirical curve using Eq. (1); closed squares, VFTRIM-3D code; upward facing triangles, Roth et al.; downward facing triangles, Roth et al. (adj. to 45°); open squares, Roth; diamonds, Roth (adj. to 45°); open circles, Bohdansky et al.; crosses, Bohdansky et al. (adj. to 45°).

6. DISCUSSION

The experiments conducted at the Max-Planck-Institut für Plasmaphysik (IPP) are the only other source of experimental data, as noted in the Introduction. The data most closely corresponding to these experiments are shown in Fig. 2. Since none of these points were taken at 45°, the values were adjusted with Yamamura's formula [41],

$$Y(E_0,\alpha) = Y(E_0,\alpha = 0°)(\cos\alpha)^{-f} \times \exp\{f[1-(\cos\alpha)^{-1}]\}\cos\alpha_{\text{opt}}.$$

These data are plotted in Fig. 2 along with the data from this study. The latter match the IPP data fairly well in the 300 eV case, in that the IPP data lie above and below the data from this experiment. A few features of the IPP data should be evident, however. The data shown here represent various experiments conducted between 1985 and 1989 [42–44]. There is significant spread in the values at both 100 and 300 eV, even for values published in the same article. This underscores the difficulty of these measurements and the need for additional work in this area. The few values that exist below 100 eV are in general higher than

Table II. Fit to a $\cos^n(\Theta)$ Distribution for D^+ Ions Incident on Beryllium at 45[ffi] to the Normal

Energy (eV)	n
20	0.67 ± 0.14
50	0.70 ± 0.12
100	0.72 ± 0.15
300	0.80 ± 0.14
500	0.85 ± 0.11
700	0.91 ± 0.16

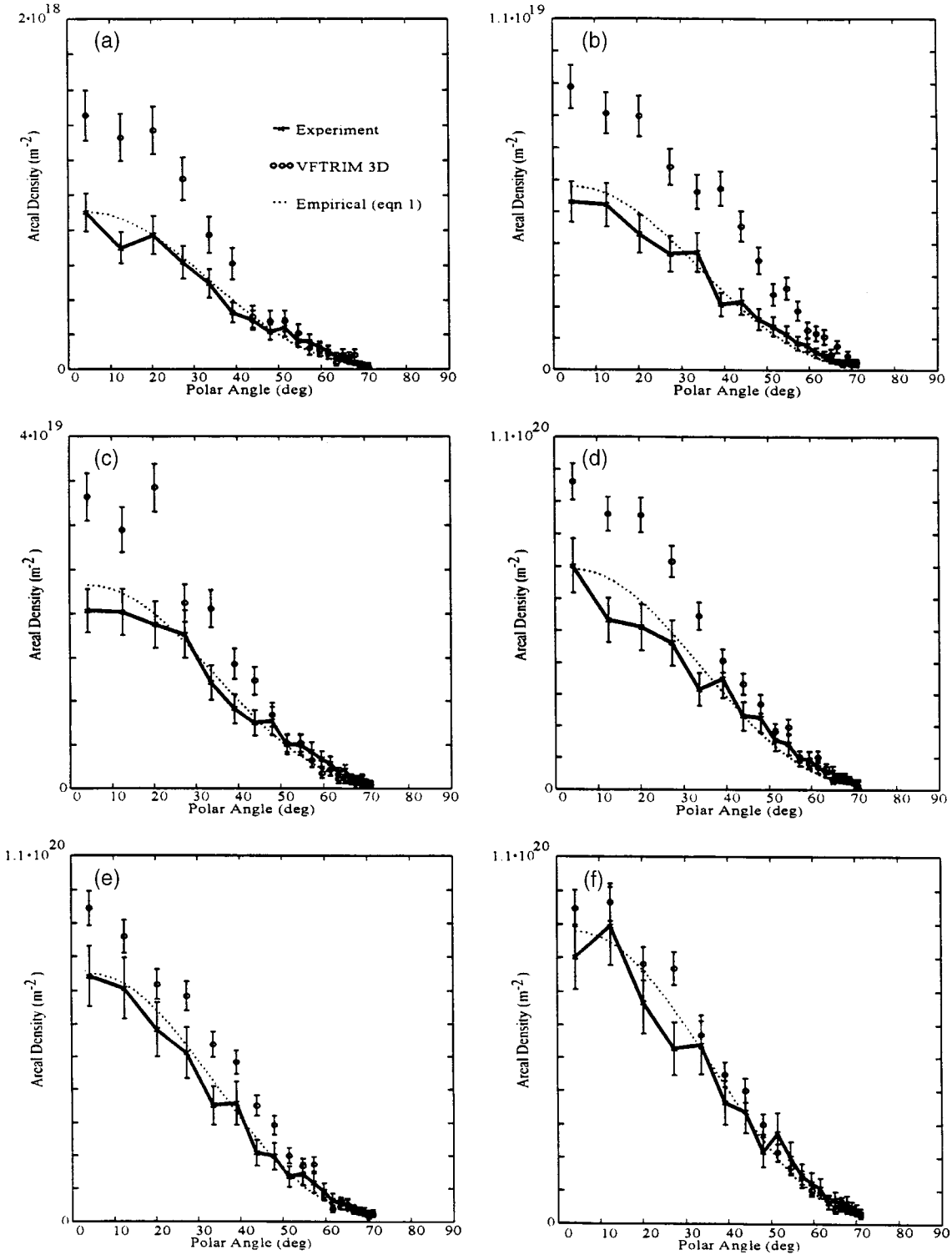

FIG. 3. Angular distribution of material on the collector plate for a D^+ ion beam incident on a beryllium sample at 45° to the normal: (a)–(f).

the data presented here, the VFTRIM-3D data, and the empirical formula developed at IPP. Yamamura's scaling formula, which should correct for the angle of incidence, clearly fails in the case of the 300 eV 50° data when compared with the 300 eV 0° case. Although one would expect the yields to be similar once corrected for angle of incidence, the 300 eV 0° case appears to be approximately 50% lower than expected. The empirical sputtering formula explained in Section 2 gives values that are close at low energies but tend to be low for higher energies. The implications for fusion devices are that designs based on the empirical formula are likely to underestimate the sputtering yield due to D^+ on beryllium.

The low energy data show sputtering at lower levels than previously observed and, more importantly, sputtering at 10 eV was detected even though this is below the calculated threshold energy of 13.25 eV predicted by the following equation [19]:

$$E_{\text{th}} = E_{\text{s}} \left[7.0 \left(\frac{M_2}{M_1} \right)^{-0.54} + 0.15 \left(\frac{M_2}{M_1} \right)^{1.12} \right].$$

This equation was an extension of an analytical model that had been empirically fitted. Several mechanisms could explain this. For example, the formation of beryllium carbides or hydrides at the surface could lower the binding energy. In addition, the surface texture could result in atoms located on peak features, for example, having lower binding energies than those in the bulk material. Molecular dynamics simulations also suggest that there are mechanisms in which the sputtered particle is hit more than once, resulting in a larger momentum transfer. Finally, this experiment measures extremely low amounts of sputtering, and data of this kind were not available to properly scale the empirical yield formula.

The angular distributions of the sputtered material are not surprising. They are slightly undercosine as shown in Table II, increasing to nearly cosine at 700 eV. This indicates that at the lower energies a large majority of the interactions are very near the surface. Had deeper interactions been very significant, the distribution would have been overcosine.

Several features of the distribution suggest the possibility of structure beyond a simple cosine distribution. For example, there are dips in the distribution for 20 eV at 12°, 50 eV at 39°, 300 eV at 34°, 500 eV at 34° and 700 eV at 4°. These features seem significant when compared with the error bars, but their occurrence at various points in the distribution suggests that they are not physical. Another feature of the distribution is the correlation between the experimental distribution and the VFTRIM-3D distribution. As the energy increases from 20 to 700 eV the fit between the simulation and the experiment improves dramatically. This is not surprising given the fact that one of the purposes of this article is to provide data to allow these codes to function more accurately at lower energies.

7. CONCLUSIONS

The experimental apparatus and procedure described herein have been demonstrated to obtain data characterizing the sputtering yield and the angular distribution for 10 to 700 eV D^+ on beryllium at 45° to the normal. Issues of surface preparation have been addressed with the implementation of in situ plasma cleaning of the samples and a vacuum transfer system. This beryllium dataset is the first of its kind at these low energies and is only the second set of data available for D^+ on beryllium at all [17]. The previous data are virtually all for normally incident ions and the scatter in these data points (Fig. 2) illustrates the need for more work in this area. At low energies, where conventional sputtering theories break down, these experiments can provide data that will help shape and confirm new theories of low energy ion–surface interaction. A better understanding of these processes may lead to the development of plasma facing components with enhanced lifetimes and reduced contamination of fusion plasmas.

REFERENCES

[1] GAUSTER, W.B., SPEARS, W.R., ITER JOINT CENTRAL TEAM, in Atomic and Plasma–Material Interaction Data for Fusion (Suppl. to Nucl. Fusion), Vol. 5, IAEA, Vienna (1994) 7.
[2] ROTH, J., J. Nucl. Mater. **176&177** (1990) 132.
[3] POST, D.E., BEHRISCH, R., STANSFIELD, B., in Physics of Plasma Wall Interactions in Controlled Fusion, NATO ASI Series B: Physics, Vol. 131 (POST, D.E., BEHRISCH, R., Eds), Plenum Press, New York and London (1984) 1.
[4] ISLER, R.C., Nucl. Fusion **24** (1984) 1599.
[5] ROTH, J., VIETZKE, E., HAASZ, A.A., in Atomic and Plasma–Material Interaction Data for Fusion (Suppl. to Nucl. Fusion), Vol. 1, IAEA, Vienna (1991) 63.
[6] DAVIS, J.W., HAAZ, A.A., STANGEBY, P.C., J. Nucl. Mater. **145–147** (1987) 417.

[7] THOMAS, P.R., JET TEAM, J. Nucl. Mater. **176&177** (1990) 3.
[8] ITER Conceptual Design, ITER Documentation Series, No. 7, IAEA, Vienna (1990).
[9] BILLONE, M.C., DALLE DONNE, M., MACAULAY-NEWCOMBE, R.G., "Status of beryllium development for fusion applications", Fusion Nuclear Technology (Proc. 3rd Int. Symp. Los Angeles, 1994).
[10] HWANG, A., et al., J. Nucl. Mater. **176&177** (1990) 588.
[11] WILSON, K.L., et al., in Atomic and Plasma–Material Interaction Data for Fusion (Suppl. Nucl. Fusion), Vol. 1, IAEA, Vienna (1991) 161.
[12] MACAULAY-NEWCOMBE, R.G., J. Nucl. Mater. A **191–194** (1992) 263.
[13] WAMPLER, W.R., J. Nucl. Mater. **196–198** (1992) 981.
[14] HECHTL, E., ROTH, J., ECKSTEIN, W., WU, C.H., J. Nucl. Mater. **220–222** (1995) 883.
[15] BROOKS, J.N., RUZIC, D.N., HAYDEN, D.B., TURKOT, R.B., Jr., J. Nucl. Mater. **220–222** (1995) 269.
[16] HIROOKA, Y., WON, J., BOIVIN, R., SZE, D., NEUMOIN, V., J. Nucl. Mater. **228** (1996) 148.
[17] ECKSTEIN, W., GARCÍA-ROSALES, C., ROTH, J., OTTENBERGER, W., Sputtering Data, Max-Planck-Institut für Plasmaphysik, Garching (1993).
[18] BORDERS, J.A., LANGLEY, R.A., WILSON, K.L., J. Nucl. Mater. **76** (1978) 168.
[19] GARCÍA-ROSALES, C., ECKSTEIN, W., ROTH, J., J. Nucl. Mater. **218** (1994) 8.
[20] GAUTHIER, E., ECKSTEIN, W., LASZLO, J., ROTH, J., J. Nucl. Mater. **176&177** (1990) 438.
[21] WHITLEY, J.B., WILSON, K.L., BUCHENAUER, D.A., J. Nucl. Mater. A **255–257** (1998) 82.
[22] ROTH, J., ECKSTEIN, W., GAUTHIER, E., LASZLO, J., J. Nucl. Mater. A **179–181** (1991) 34.
[23] SMITH, P.C., Low-Energy Angularly-Resolved Sputtering Measurements, PhD Thesis, Dept. of Nuclear Engineering, Univ. of Illinois, Urbana-Champaign (1997).
[24] RUZIC, D.N., SMITH, P.C., TURKOT, R.B., Jr., J. Nucl. Mater. **241–243** (1997) 1170.
[25] BROOKS, J.N., CAUSEY, R., FEDERICI, G., RUZIC, D.N., J. Nucl. Mater. **241–243** (1997) 294.
[26] BROOKS, J.N., RUZIC, D.N., HAYDEN, D.B., Sputtering erosion of Be-coated plasma facing components — general considerations and analysis for ITER detached plasma regime, J. Fusion Eng. Des. (in press).
[27] BOHDANSKY, J., Nucl. Instrum. Methods B **2** (1984) 587.
[28] BIERSACK, J., HAGGMARK, L., Nucl. Instrum. Methods **174** (1980) 252.
[29] BIERSACK, J., ECKSTEIN, W., Appl. Phys. A **34** (1984) 73.
[30] TURKOT, R.B., Plasma–Material Interactions: A Langmuir Probe Analysis of a Cylindrical SiO_2 Deposition System and a Computational Study Using VFTRIM-3D, PhD Thesis, Dept. of Nuclear Eng., Univ. of Illinois, Urbana-Champaign (1996).
[31] SHAHEEN, M.A., RUZIC, D.N., J. Vac. Sci. Technol., A Vac. Surf. Films **11** (1993) 3085.
[32] RUZIC, D.N., Plasma Sci. **24** (1996) 81.
[33] WAMPLER, W.R., J. Nucl. Mater. **122&123** (1984) 1598.
[34] KAWAMURA, H., et al., J. Nucl. Mater. **176&177** (1990) 661.
[35] CHODURA, R., in Physics of Plasma Wall Interactions in Controlled Fusion, NATO ASI Series B: Physics, Vol. 131 (POST, D.E., BEHRISCH, R., Eds), Plenum Press, New York and London (1984).
[36] WAHLIN, L., Nucl. Instrum. Methods **27** (1964) 55.
[37] MENZINGER, M., WAHLIN, L., Rev. Sci. Instrum. **40** (1969) 102.
[38] DAHL, D.A., SIMION3D Version 6.0, Lockheed Martin Idaho Technologies, Idaho Natl Engineering Lab., Idaho Falls (1995).
[39] SAUERBREY, G.Z., Z. Phys. **155** (1959) 206.
[40] SEAH, M.P., "Quantification of AES and XPS", Practical Surface Analysis, Vol. 1 (BRIGGS, D., SEAH, M.P., Eds), (1990).
[41] YAMAMURA, Y., ITIKAWA, Y., ITOH, N., Angular Dependence of Sputtering Yields of Monoatomic Solids, Rep. IPPJ-AM-26, Nagoya Univ. (1983).
[42] ROTH, J., ECKSTEIN, W., BOHDANSKY, J., J. Nucl. Mater. **165** (1989) 199.
[43] ROTH, J., J. Nucl. Mater. **145–147** (1987) 87.
[44] BOHDANSKY, J., ROTH, J., OTTENBERGER, W., Sputtering Measurements of Beryllium, Rep. IPP-JET No. 31, Max-Planck-Institut für Plasmaphysik, Garching (1985).

(Manuscript received 16 July 1997
Final manuscript accepted 29 January 1998)

E-mail address of D.N. Ruzic:
druzic@uiuc.edu

Subject classification: I0, Ge; I0, Gt